



Published in final edited form as:

*Mol Cell*. 2015 July 16; 59(2): 163–175. doi:10.1016/j.molcel.2015.05.038.

## A major role of DNA polymerase $\delta$ in replication of both the leading and lagging DNA strands

Robert E. Johnson<sup>#1</sup>, Roland Klassen<sup>#1,3</sup>, Louise Prakash<sup>1,\*</sup>, and Satya Prakash<sup>1</sup>

<sup>1</sup>Department of Biochemistry and Molecular Biology, University of Texas Medical Branch, Galveston, TX 77555-1061, USA

# These authors contributed equally to this work.

### SUMMARY

Genetic studies with *S. cerevisiae* Pol $\delta$  (*pol3-L612M*) and Pol $\epsilon$  (*pol2-M644G*) mutant alleles, each of which display a higher rate for the generation of a specific mismatch, have led to the conclusion that Pol $\epsilon$  is the primary leading strand replicase and that Pol $\delta$  is restricted to replicating the lagging strand template. Contrary to this widely accepted view, here we show that Pol $\delta$  plays a major role in the replication of both DNA strands, and that the paucity of *pol3-L612M* generated errors on the leading strand results from their more proficient removal. Thus, the apparent lack of Pol $\delta$  contribution to leading strand replication is due to differential mismatch removal rather than differential mismatch generation. Altogether, our genetic studies with Pol3 and Pol2 mutator alleles support the conclusion that Pol $\delta$ , and not Pol $\epsilon$ , is the major DNA polymerase for carrying out both leading and lagging DNA synthesis.

### INTRODUCTION

A number of models have been proposed for the roles of DNA polymerases (Pol $\delta$  and  $\epsilon$ ) in the replication of the two DNA strands. A role for Pol $\delta$  in the replication of both DNA strands was indicated from studies of SV40 replication (Tsurimoto and Stillman, 1991a; Tsurimoto et al., 1990; Tsurimoto and Stillman, 1991b; Waga and Stillman, 1994). The observations that the DNA polymerase activity of Pol $\epsilon$  is not essential (Feng and D'Urso, 2001; Kesti et al., 1999; Suyari et al., 2012) whereas the polymerase function of Pol $\delta$  is indispensable for viability (Boulet et al., 1989; Hartwell, 1976; Simon et al., 1991; Sitney et al., 1989), also supported a role for Pol $\delta$  as the major replicase. However, more recent genetic studies with error-prone variants of yeast Pol $\delta$  and Pol $\epsilon$  led to a model whereby Pol $\epsilon$  primarily replicates the leading DNA strand and Pol $\delta$  replicates the lagging strand (Larrea et

\*Correspondence: s.prakash@utmb.edu.

<sup>3</sup>Present address: Institut für Biologie, FG Mikrobiologie, Universität Kassel, Kassel D-34132, Germany roland.klassen@uni-kassel.de

**Publisher's Disclaimer:** This is a PDF file of an unedited manuscript that has been accepted for publication. As a service to our customers we are providing this early version of the manuscript. The manuscript will undergo copyediting, typesetting, and review of the resulting proof before it is published in its final citable form. Please note that during the production process errors may be discovered which could affect the content, and all legal disclaimers that apply to the journal pertain.

### SUPPLEMENTAL INFORMATION

Supplemental Information contains Experimental Procedures for the construction of mutant strains, 6 tables, and 7 figures.

al., 2010; Nick McElhinny et al., 2008; Pursell et al., 2007). This model of asymmetric leading and lagging strand replication by two different DNA polymerases is now widely accepted.

This model relies on data from *Saccharomyces cerevisiae* strains harboring the *pol3-L612M* mutation in the catalytic subunit of Pol $\delta$  or the *pol2-M644G* mutation in the catalytic subunit of Pol $\epsilon$ . From the observations indicating the prevalence of signature mutations in the lagging strand in the *pol3-L612M* and the *pol3-L612M msh2* mutant strains, a role for Pol $\delta$  in the replication of the lagging strand was inferred (Nick McElhinny et al., 2008). And from the prevalence of signature mutations in the leading strand in the *pol2-M644G* mutant, a role for Pol $\epsilon$  in the replication of the leading strand was deduced (Pursell et al., 2007).

Mismatched base pairs generated during DNA synthesis by the replicative Pols are removed by multiple processes including mismatch repair (MMR), Exo1, and proofreading by the 3'  $\rightarrow$ 5' exonuclease activities of Pol $\delta$  and Pol $\epsilon$ . Hence, the relative prevalence of signature mutations on the two DNA strands could be affected by either differential rates of error generation during replication or by the differential action of mismatch removal processes on the two DNA strands. In view of these considerations, we re-examined the roles of Pols  $\delta$  and  $\epsilon$  in the replication of the two DNA strands and show that MMR, as well as Exo1 and Pol $\epsilon$  exonuclease, compete for the removal of replication errors on both the DNA strands, and that differential error removal rather than differential mismatch generation accounts for the bias of replication errors on the lagging strand in the *pol3-L612M* strain.

Furthermore, the complete absence of Pol $\epsilon$  signature mutations from the leading strand in the *pol2-M644G msh2* strain supports the conclusion that the DNA polymerase activity of Pol $\epsilon$  does not significantly contribute to DNA synthesis on the leading strand. In addition to its well-established essential non-catalytic role as a component of the CMG helicase complex, we propose an important role for Pol $\epsilon$  proofreading exonuclease in the removal of Pol $\delta$  generated errors from the leading DNA strand, and suggest that this Pol $\epsilon$  role can account for all the observations that have been used to implicate a role of Pol $\epsilon$  in the replication of the leading DNA strand.

## RESULTS

Pol $\delta$  L612M has reduced fidelity and exhibits significant bias for the generation of a T:dGTP mismatch which occurs 28-fold more frequently than the reciprocal A:dCTP mismatch (Nick McElhinny et al., 2007). *pol3-L612M* strains carrying a wild type *URA3* gene inserted close to *ARS306* in two different orientations in the  $[-2]-7A$ -YUN1300 genetic background display a highly asymmetric *URA3* to *ura3* hotspot mutational spectrum, wherein the T97C and G764A base substitution hot spots occurred primarily in one orientation, and the C310T hot spot occurred in the other (Nick McElhinny et al., 2008). Based on the biased fidelity of the mutant polymerase for reciprocal mismatches, these hot spots likely arose via T:dGTP (T-C mutation) and G:dTTP (G-A and C-T mutations) mispairs generated by L612M-Pol $\delta$ . Since these mutations occurred at high frequency only in the orientation where the hypermutable residue was present in the lagging strand template, Pol $\delta$  was assigned to primarily replicate the lagging strand (Nick McElhinny et al.,

2008). Among the three base change hot spots within *URA3*, the C310T substitution via a G:dTTP mispair occurs at a slightly higher rate than the others (Nick McElhinny et al., 2008) and results in a nonsense TAG codon at position 104, which we refer to as *ura3-104*. Since reversion of *ura3-104* (*amber*) back to wild type Gln-104 would require a T:dGTP insertion in the strand opposite the original G:dTTP mispair which occurred in the forward mutation (Figure S1A), we explored the possibility that the reversion of *ura3-104* would be specifically favored by L612M-Pol $\delta$ .

### ***ura3-104* Reversion In Vivo in S288C**

In vitro synthesis reactions confirmed that compared to wild type, the L612M mutant Pol3 catalytic subunit as well as the mutant Pol $\delta$  holoenzyme inserted dGTP opposite template T preferentially compared to the misinsertion of dCTP opposite template A in the *ura3-104* sequence context (Figure S2 A,B). The *ura3-104* allele containing the C310T substitution (Figure S1A) was integrated into the yeast genome between the *FUS1* and *HBN1* genes located 1.2 kb left of the highly efficient early firing ARS306 (Nieduszynski et al., 2007) either in the forward (OR1) or reverse (OR2) orientations (Figure S3A,B). 2D gel analysis confirms that ARS306 remains a highly efficient origin after integration of *URA3* in the S288C wild type yeast strain (Figure S4). Thus, in the majority of cells, replication through the *ura3-104* allele will emanate from ARS306 thereby replicating T310 on the leading strand in OR1 and on the lagging strand in OR2. In the wild type background, the *ura3-104* TAG amber codon reverts to Ura3<sup>+</sup> at a low rate of  $\sim 2.5 \times 10^{-9}$  in both orientations (Table 1). *URA3* spontaneous revertants in OR1 and OR2 displayed nearly equivalent heterogeneity of mutational events at *ura3-104* (Figure S1B, C), where in approximately 43-50% of Ura<sup>+</sup> colonies arose by T310C specific reversion of the TAG codon to CAG (Gln, wild type sequence), and 49-56% occurred by conversion to either GAG (Glu), TTG (Leu) or TCG (Ser). Only 1% (2/177) arose by conversion to AAG (Lys) and no TAC (Tyr), TAT (Tyr) or TGG (Trp) (Figure S1C) events were observed. The URA<sup>+</sup> revertant colonies harboring Gln, Glu, Leu, or Ser at position 104 exhibit a robust Ura<sup>+</sup> phenotype, whereas Ura3 Lys104 colonies were weakly Ura<sup>+</sup> (Figure S1B), explaining the low frequency of its recovery. The lack of Tyr or Trp events is likely due their being Ura<sup>-</sup> and therefore unrecoverable.

### **Biased T:dGTP Error Rates in *pol3-L612M* Strains in S288C**

Next, we analyzed the reversion frequencies of the *ura3-104* allele in the two orientations (OR1 and OR2) near ARS306 in strains that harbor the *pol3-L612M* mutator allele. Unlike in the *POL3* background where the Ura<sup>-</sup> to Ura<sup>+</sup> reversion rate is similar in both orientations, the reversion rate in the *pol3-L612M* strain is over 5-fold higher when *ura3-104* is in OR2 than in OR1, and where the *ura3* T<sub>310</sub>:dGTP mispair would form during lagging strand synthesis (Table 1). In OR2 *URA3* revertants the ratio of CAG to non-CAG mutational events rose from  $\sim 50\%$  to  $\sim 95\%$ , resulting in a 16-fold increase in the specific reversion rate of TAG to CAG in the *pol3-L612M* strain. In contrast, when *ura3-104* was in OR1 in the *pol3-L612M* strain, the CAG specific reversion rate increased only 2-fold with a corresponding increase in the occurrence of CAG vs. non-CAG events from  $\sim 40\%$  to  $\sim 60\%$  (Table 1). Thus, although the *pol3-L612M* signature is observed on the leading strand, there is a 9-fold higher rate of the signature on the lagging strand. In contrast to the TAG to CAG mutation, none of the rates of the four other detectable mutation events (GAG, TTG, TCG

and AAG) are significantly increased over wild type levels in *pol3-L612M* (Figure S3C), which is consistent with the low rate and lack of bias of L612M-Pol $\delta$  for the generation of the mismatches that lead to these mutations (Nick McElhinny et al., 2007). Based on the CAG specific reversion rates in the *POL3* and *pol3-L612M* strains when *ura3-104* is in OR2, it can be estimated that approximately 95% of the TAG to CAG mutations in *pol3-L612M* are generated via T:dGTP mismatches by L612M-Pol $\delta$  during lagging strand replication  $[(\text{rate CAG } pol3-L612M \text{ OR2} - \text{rate CAG } POL3 \text{ OR2})/(\text{rate } pol3-L612M \text{ OR2})]$ . The strong mutational bias observed for the *pol3-L612M* strains harboring the two orientations of our *ura3-104* reversion system is similar to the results that have been reported for *URA3* to *ura3* forward mutational spectra in a different strain background (Larrea et al., 2010; Nick McElhinny et al., 2008) and is consistent with a role of Pol $\delta$  in lagging strand, but not in leading strand replication.

### L612M Pol $\delta$ Generated T:dGTP Errors on the Lagging Strand in S288C

To determine the role of various mispair removal processes in the correction of T:dGMP mispairs generated by L612M-Pol $\delta$ , we analyzed the frequency and orientation bias of *ura3-104* reversion in *pol3-L612M* strains additionally carrying the *pol2-4* mutation lacking the Pol $\epsilon$  proofreading exonuclease activity (Morrison et al., 1991), the *msh2* mutation defective in MMR (Johnson et al., 1996), or a deletion of *EXO1*, which contributes to mismatch removal in collaboration with MMR (Genschel et al., 2002; Sokolsky and Alani, 2000; Tishkoff et al., 1997; Tran et al., 1999), individually and in various combinations. All double mutants, including the *pol3-L612M msh2* strain grow with no apparent defect at 30°C or 37°C and do not display sensitivity to the replication inhibitor HU (Figure S5A). The lack of any significant growth defect in the *pol3-L612M msh2* strain in the S288C genetic background was further confirmed by tetrad analysis of *POL3/pol3-L612M MSH2/msh2* diploids (Figure S5B). Among the triple mutants, the *pol3-L612M pol2-4 exo1* mutant exhibits the same growth phenotype as the double mutants, while the *pol3-L612M msh2 exo1* and *pol3-L612M msh2 pol2-4* strains display a slow growth phenotype at 30°C and an inability to grow at 37°C (Figure S5A). Growth defects are more severe for the *pol3-L612M msh2 pol2-4* strain than for the *pol3-L612M msh2 exo1* strain, and both strains exhibit increased sensitivity to HU (Figure S5A). With the exception of *pol3-L612M msh2 pol2-4*, we were able to analyze reversion rates and sequence the mutational events at the *ura3-104* amber codon in all of the strains.

In OR2, where the T:dGTP mismatch occurs during lagging strand synthesis, both the *exo1* and *msh2* mutations strongly increase the CAG specific reversion rate, while *pol2-4* on its own has no effect (Table 1, Figure 1A,B). In both the *pol3-L612M exo1* and *pol3-L612M msh2* strains, the ratio of CAG versus non-CAG revertants remains strongly biased towards CAG, with non-CAG revertants occurring less than 7% (Table 1). Therefore, Exo1 and MMR efficiently remove T:dGTP mispairs made by L612M-Pol $\delta$  during lagging strand synthesis and the generation of this mispair largely outnumbers the other detectable ones, as expected by the biochemical properties of the mutant polymerase. In the *pol3-L612M msh2 exo1* strain, CAG reversion rates in OR2 were not significantly higher than in *pol3-L612M msh2* (Table 1, Figure 1A,B), supporting the view that the T:dGTP mispair correcting activity of Exo1 seen in this assay on the lagging strand occurs in the context of *MSH2*-

dependent MMR. The *pol2-4* exonuclease mutation alone did not increase either the total rate or the CAG specific reversion rate of *ura3-104* by *pol3-L612M*. However, *pol2-4* significantly increased the CAG reversion rate in combination with the *exo1* mutation in the *pol3-L612M* strain (*pol3-L612M pol2-4 exo1* OR2; Table 1, Figure 1A,B), suggesting that Polε exonuclease can be recruited to the lagging strand to remove T:dGTP errors generated by Polδ, but that its absence alone can be compensated for by other mismatch removal processes.

### L612M-Polδ Generated T:dGTP Errors on the Leading Strand in S288C

Next, we examined the effects of *pol2-4*, *msh2*, and *exo1*, alone or in different combinations, on the reversion rates in *pol3-L612M ura3-104* OR1, where the T:dGTP mismatch occurs during leading strand synthesis. While the *pol2-4* mutation did not increase the overall *ura3-104* reversion rate, the ratio of CAG to non-CAG events rose dramatically from ~ 60% to 100% (Table 1) leading to an increase the CAG-specific reversion rate, suggesting that proofreading by Polε participates in the removal of some *pol3-L612M* generated T to C signature errors on the leading strand. The *exo1* mutation conferred a 6-fold increase in CAG reversion rate over the level seen in *pol3-L612M* alone (Table 1; Figure 1A,B). Strikingly, however, the combined absence of Exo1 and Polε exonuclease (*pol3-L612M pol2-4 exo1*) caused an ~85-fold increase in CAG reversion rate, and in a sample size of 123, no non-CAG events were detected (Table 1, Figure 1B). The strong increase of the CAG-specific reversion rate of *ura3-104* in OR1 along with the very low (undetectable) *ura3-104* amber reversion rate via non-T:dGTP errors (GAG, TTG, TCG and AAG revertants) indicates that L612M-Polδ generates a very considerable amount of replication errors on the leading strand which becomes detectable only after removal of both Polε proofreading and Exo1. Therefore, the proofreading activity of Polε and Exo1 represent redundant functions that remove T:dGTP mismatches generated by L612M Polδ on the leading strand. When CAG-specific reversion rates in OR1 and OR2 are compared, the strong ~9 fold bias towards T:dGTP mismatches occurring on the lagging strand that was observed in *pol3-L612M* alone becomes greatly weakened in *pol3-L612M pol2-4 exo1* (Figure 1C) to only about 2-fold. Since the *exo1* mutation confers a much weaker mutation phenotype than *msh2*, and *MSH2*-dependent MMR remains functional in *exo1* (Tran et al., 1999), the fact that the T:dGTP error rate remains biased on the lagging strand could be due to Exo1 independent MMR being more effective on the leading than on the lagging strand. As discussed below, the results obtained with *msh2* support this possibility.

Inactivation of MMR by *msh2* in *pol3-L612M* conferred ~370-fold increase in the CAG reversion rate of *ura3-104* (OR1), and the additional removal of Exo1 (*pol3-L612M msh2 exo1*) elevated the CAG reversion rate to ~470-fold over the level seen in *pol3-L612M ura3-104* (OR1) (Table 1; Figure 1B). In both cases, the frequency of non-CAG revertants becomes ~2%, indicating again that the large increase in mutation rates is due to the specific T310:dGTP mispair incorporation by L612M-Polδ during replication of the leading strand which, under normal circumstances, are removed by MMR. Interestingly, the orientation bias in which more T:dGTP errors occur during lagging strand synthesis (OR2) in *pol3L612M MSH2* is reversed in *pol3-L612M msh2*, where the CAG-specific reversion rate becomes ~2.5 fold higher for T:dGTP mismatch incorporation on the leading strand

(OR1) (Table 1; Figure 1C). This result indicates that in the S288C-isogenic strain, MMR is highly effective in the removal of the T:dGTP mismatch at T310 of the *ura3-104* allele on the leading strand. Thus, the higher lagging strand T:dGTP error rate in *pol3-L612M MSH2* was due to biased leading strand MMR rather than biased lagging strand error generation. Since the removal of both Exo1 and Msh2 further elevated CAG reversion rates in *pol3-L612M ura3-104* in OR1, which also increased the OR1/OR2 bias further towards the leading strand error (Table 1; Figure 1C), a function of Exo1 independent MMR on the leading strand cannot be excluded entirely.

### **Lack of L612M Pol $\delta$ Mutational Bias in the Replication of Leading and Lagging Strands: Analysis of Forward Mutations in *URA3* in S288C**

Our analysis of *ura3-104* reversion near ARS306 in the *pol3-L612M* strain in the absence of different mismatch removal processes has provided strong evidence that Pol $\delta$  generates replication errors on both the leading and lagging DNA strands in the S288C strain background. To further confirm this, we carried out forward mutational analyses of *URA3* near ARS306. For each *pol3-L612M* and *pol3-L612M msh2* strain harboring the *ura3-104* allele in OR1 or OR2, the mutant *ura3-104* allele was reverted to the wild type CAG codon by direct transformation with a DNA fragment containing the *URA3* wild type sequence. In the *pol3-L612M* OR1 and OR2 strains, the *URA3* to *ura3* forward mutation rates were similar,  $1.8 \times 10^{-7}$  and  $1.5 \times 10^{-7}$ , respectively (Table S1). Sequence analysis of mutations arising in OR1 and OR2, however, was suggestive of lagging strand mutation bias in accordance with L612M Pol $\delta$  signatures. For instance, C310T mutations, which are predicted to arise from biased G:dTTP mispair generation, were observed in 10 out of 71 mutational events in OR1 (G in lagging), whereas none occurred at this position in 78 mutational events in OR2 (G in leading). Conversely, 9 of 78 mutations in OR2 were T97C mutations (T in lagging), whereas none occurred at this position in OR1 (T in leading). Although in the previous study, the G764A hot spot mutation occurred in an orientation dependent fashion (Nick McElhinny et al., 2008), in our *pol3-L612M* strains, we observed only 2/71 and 5/78 G764A mutations in OR1 and OR2, respectively, and the overall rate of G to A mutations was only 1.4 $\times$  higher in OR2 (G in lagging) than in OR1 (G in leading). All other mutational events observed were either not correlated to the L612M Pol $\delta$  signature, or did not exhibit orientation bias. However, despite lack of bias for G to A mutations, the occurrence of the C310T and T97C hot spots is consistent with the previous study (Nick McElhinny et al., 2008), and together with our mutational analysis of *ura3-104* reversion in the *pol3-L612M* strain, they indicate a prevalence of L612M Pol $\delta$  signature errors on the lagging strand when MMR is proficient.

Next we analyzed *URA3* to *ura3* forward mutations that occur in the *pol3-L612M msh2* strain in OR1 and OR2 orientations in the S288C genetic background. MMR efficiently repairs 1 basepair frameshifts, and in the previous study (Nick McElhinny et al., 2008), three orientation specific  $-1$  frameshift hot spots (A174-178, T201 - 205, T255-260) occurred in *URA3* in the *pol3-L612M msh2* strain and were assigned to L612M Pol $\delta$  synthesis by correlation to an 11:1 bias for deletions of T over deletions of A (Nick McElhinny et al., 2007). Similar to the *pol3-L612M* single mutant strain, the base changes that dominated the mutation spectra in the *pol3-L612M msh2* strain were the T97C, C310T, and G764A

hotspots. Based upon the remarkable asymmetry with which these mutations arose in the two different orientations, and based upon the biased mispair formation spectra of L612M Pol $\delta$ , the high mutation rates of these hot spots were assigned to have arisen from errors made during lagging strand replication. (Nick McElhinny et al., 2008; Nick McElhinny et al., 2007).

For our analyses, we used the same procedure to calculate the leading and lagging strand mutation rates at each hot spot as was used in the previous study (Nick McElhinny et al., 2008). At each hot spot, the proportion of mutations generated in each strand was calculated based on the reciprocal mismatch bias of L612M Pol $\delta$  (Figure 2A) as determined from mutations generated during DNA synthesis on a *lacZ* substrate (Nick McElhinny et al., 2007). The number of mutations assigned to each strand was divided by the total mutations sequenced and then multiplied by the total mutation rate to give the strand specific mutation rate for each site (Table S2, Figure 2B,C). In OR2 where the coding sequence is in the lagging strand, we observe the signature T97C and G764A hot spots (Figure 2C), and these hot spots do not occur in OR1 at any significant rate (Figure 2B); however, we do observe the G to A mutations at C310 in OR2 (Figure 2C) that would arise from errors made during leading strand replication. In addition, whereas T(-1) hot spots were observed to occur almost exclusively in the lagging strand in the previous study (Nick McElhinny et al., 2008), we observe frameshift hot spots occurring in both the DNA strands. For instance, in OR2, frameshifts at T(201-205) or T(255-260), which would arise during lagging strand synthesis, occur each at a rate of  $\sim 4 \times 10^{-7}$ , whereas frameshifts at A(174-178), where the T run is in the leading strand, occur at a rate of  $\sim 2 \times 10^{-7}$  (Figure 2C). And in OR1, where T(255-260) occurs in the leading strand, the frameshifts occur at a rate of  $\sim 1.5 \times 10^{-7}$  (Figure 2B). Finally, we observe two orientation specific G to T hot spot mutations (G679 and G706) that occur at rates 34 $\times$  and 15 $\times$  higher in OR1 than in OR2, that were not observed in the previous study (Nick McElhinny et al., 2008). Importantly, L612M Pol $\delta$  exhibits an 8.5:1 bias for G:dATP mispair formation over the C:dTTP mispair (Nick McElhinny et al., 2007), and we have confirmed that at position 679 in *URA3*, L612M Pol3 exhibits preferential incorporation of an A opposite template G compared to the incorporation of a T opposite template C (Figure S2C,D). Therefore, since  $\sim 90\%$  of G679T and G706T hotspot mutations can be attributed to having occurred from a G:dATP mispair, the high rate of these two hot spot mutations occurring in OR1 can be assigned to errors made by Pol $\delta$  during leading strand replication. When OR1 and OR2 strand specific mutation rates are compared, the total *pol3-L612M* signature hot spot mutation rate of *URA3* in OR1 is  $\sim 3$  fold higher in the leading strand than in the lagging strand (Figure 2B); while in OR2, the total *Pol3-L612M* signature hot spot mutation rate is  $\sim 3$  fold higher in the lagging strand than in the leading strand (Figure 2C).

### Analysis of Forward Mutations in *URA3* Integrated at Three Different Genomic Locations in the DBY747 Strain

To determine whether our observations were unique to the S288C genetic background or shared by other yeast strains, we examined *URA3* forward mutations in OR1 and OR2 at ARS306 and ARS1 in the DBY747 strain harboring the *pol3-L612M msh2* mutations. In this strain, the genomic copy of *URA3* was deleted to prevent rearrangements with the *URA3*

gene integrated near an ARS. In addition to integrating the *URA3* gene in opposite orientations (OR1 and OR2) ~1.2 kb left of ARS306 as was done in the S288C strain, the *URA3* was also integrated in opposite orientations at a second position on chromosome 3, ~10kb left of ARS306, located in the intergenic region between the *STE50* and *RRP7* genes. In the DBY747 genetic background also we observed no growth defect in the *pol3-L612M msh2* double mutant strain. In this strain we find that, regardless of whether *URA3* was located 1.2 kb or 10 kb left of ARS306 on chromosome 3, individual hotspot mutation sites were far less orientation specific than observed in the S288C background (Tables S3 and S4, Figures 3 and 4). For instance, even though ~74-80% of all mutations still correlated with the L612M Pol $\delta$  signatures, the base change hotspot at C310T was observed in both OR1 and OR2 (Figures 3 and 4). By contrast, the hotspot mutation T97C was evident in OR1 at 1.2 kb left of ARS306, whereas none were observed in OR2 at this position (Figure 3). Frameshift mutation hotspots remain highly localized to positions A174-178, T201-205 and T255-260, yet the rates of each are nearly equal in both orientations (Tables S3, S4, Figures 3 and 4). When the numbers of mutations are allocated to the leading and lagging strands based on the bias of L612M Pol $\delta$  enzyme and the rates are compared, in either orientation, the rates of *URA3* hotspot mutations on the two DNA strands are nearly identical. For example, at 1.2 kb left of ARS306, the -1 frameshift mutation rate at T255-260 was  $1.32 \times 10^{-7}$  on the leading strand in OR1, and  $1.66 \times 10^{-7}$  on the lagging strand in OR2 (Figure 3). Similarly, at 10kb left of ARS306, the T255-260 -1 frameshift rates were  $1.09 \times 10^{-7}$  on the leading strand in OR1, and  $1.16 \times 10^{-7}$  on the lagging strand in OR2 (Figure 4). The only bias observed was at 1.2 kb left of ARS306 in which there was a ~2.5 fold higher rate of C310T mutations in the lagging strand in OR1 over leading strand mutations in OR2 (Figure 3). When the total *pol3-L612M* dependent hotspot mutation rates are compared in either OR1 or OR2 at 1.2kb or 10kb left of ARS306, the hotspot mutation rates are nearly identical on the leading and lagging strands (Figures 3 and 4).

To further verify the role of Pol $\delta$  in the replication of the two DNA strands in the DBY747 *pol3-L612M msh2* strain, we examined forward mutations of *URA3* when integrated near another highly efficient early firing origin, *ARS1*, located on chromosome 4 (Nieduszynski et al., 2007). In this strain also, hot spot mutations occur in both the DNA strands in OR1 and OR2 (Table S5, Figure 5). Overall, in OR1, the leading strand mutation rate of  $3.5 \times 10^{-7}$  was slightly higher than the lagging strand rate of  $2.9 \times 10^{-7}$ , and in OR2, the lagging strand hotspot mutation rate of  $7.5 \times 10^{-7}$  was only 1.7 fold higher than rate of  $4.5 \times 10^{-7}$  in the leading strand (Figure 5).

Thus, at both ARS306 and ARS1 in the S288C and DBY747 strains in the *pol3-L612M msh2* genetic background, although there are some *pol3-L612M* dependent *URA3* hot spot mutations that occur in an orientation-dependent manner, we do not observe the lagging strand specificity of L612M Pol $\delta$  signature mutations; rather, we find that L612M Pol $\delta$  dependent signature hot spot mutations occur on both DNA strands of *URA3*.

### Pole Role in Leading Strand Replication

In view of the strong evidence that L612M Pol $\delta$ -generated errors occur on both the DNA strands, and that various mismatch removal processes can affect leading strand errors, we



reevaluated the evidence for Pol $\epsilon$ 's role in leading strand replication. The latter was inferred from orientation biased *URA3* error rates and mutation spectra of a *pol2-M644G* mutator allele of Pol $\epsilon$ . M644G-Pol $\epsilon$  generates a T:dTTP mismatch ~40-fold over the reciprocal A:dATP mismatch (Pursell et al., 2007).

First, we examined whether the *pol2-M644G* mutator allele has similar effects on the *URA3* forward mutation spectra in the S288C genetic background. Our *pol2-M644G* strain with intact MMR exhibits a similar *ura3* mutation profile (Figure 6) to the yeast strain used in the previous study (Pursell et al., 2007). For instance, 72% (54 out of 75) of *ura3* mutants were due to A to T mutations at the A279 and A686 hot spots when the orientation of *URA3* was such that the non-coding strand T was in the leading strand (OR2) (Figure 6A,B). When *URA3* is in the opposite orientation (OR1), however, no hot spot mutations were observed among 43 *ura3* mutants examined, but there is a slight bias for T to A mutations, consistent with T:dTMP mispairs being made in the leading strand in this orientation as well. Overall, T:dTMP mispair formation is biased for the leading strand 61:1 in OR2 and 9:1 in OR1 (Figure 6A,B). Thus, these data are consistent with the previous report (Pursell et al., 2007) and could indicate that M644G-Pol $\epsilon$  generates T:dTTP mismatches on the leading strand, but not on the lagging strand. However, since our results with *pol3-L612M* show that MMR and other mismatch removal processes can affect the observed bias for signature mutations on both strands (Tables 1, S1, and S2, Figures 1 and 2), we examined how MMR affects the orientation bias of the two hot spots generated by *pol2-M644G* (Figure 6). Surprisingly, in the *pol2-M644G msh2* strain containing *URA3* OR2, where the M644G Pol $\epsilon$  mutation signature is expected to become higher than in the *pol2-M644G* strain, we observed no hot spot mutations at A279 or A686 in 81 spontaneous *ura3* mutants analyzed (Figure 6A, C). Additionally, A to T and T to A changes occur in only 7% of mutants (6 out of 81) (Figure 6A), and even in these limited cases, the A to T bias is toward mutations generated in the lagging strand. Overall, in the *pol2-M644G msh2* strain, we could not detect any *pol2-M644G* signature mutations on the leading strand in the *URA3* gene.

Since there is no orientation dependent bias in the A to T and T to A mutations detected in *pol2-M644G msh2* and both of these events are rare compared to other base changes, there is no evidence for Pol $\epsilon$  having a significant replicative role on either the leading or the lagging strand. Our observation that A-T and T-A errors are infrequent in the *msh2* strain that harbors M644G-Pol $\epsilon$ , which has been shown to exhibit a high error rate for T:dTTP mismatches *in vitro* (Pursell et al., 2007), is consistent with the interpretation that Pol $\epsilon$  has, at best, a minor DNA synthesis role during normal DNA replication.

## DISCUSSION

### Roles of Pol $\epsilon$ Exonuclease, Exo1, and MMR in Removing Pol $\delta$ Errors from Leading and Lagging Strands

The results of our *ura3-104* reversion assay show that signature errors of *pol3-L612M* on the two DNA strands are modulated differentially by mismatch removal processes. For instance, although neither *pol2-4* nor *exo1* strongly increased L612M Pol $\delta$ 's signature error accumulation on the leading strand, the combination of both did so to a large extent (Table 1). On the lagging strand, however, *exo1* alone substantially increased L612M Pol $\delta$ -

dependent error accumulation and only a modest further increase occurred in combination with *pol2-4*. Therefore, Pol $\epsilon$  exonuclease and Exo1 act redundantly in error-editing on the leading strand, whereas Exo1-dependent mismatch correction is more prevalent on the lagging strand. Additionally, MMR has a very prominent role in correcting L612M Pol $\delta$  errors from the leading strand (Table 1). Thus, differential error removal rather than differential mismatch generation accounts for the bias of lagging strand errors observed in the *pol3-L612M* strain (Table 1, Figure 1).

### Role of MMR in Removing Errors from the Leading and Lagging Strands in Different Yeast Strains

Our analyses of *URA3* to *ura3* forward mutations in the S288C and DBY747 *pol3-612M msh2* strains provide additional support for the role of MMR in the correction of L612M Pol $\delta$ -generated errors on the leading strand. In the S288C background, whereas signature mutations are observed primarily on the lagging strand in the *pol3-L612M* strain (Table S1), signature errors occur on both strands in the *pol3-L612M msh2* strain (Table S2, Figure 2). Although in the *pol3-L612M msh2* strain the L612M Pol $\delta$ -generated hot spot mutations occur on both DNA strands, the sites at which specific hot spots occur differ in an orientation-dependent manner. This indicates that both MMR and L612M-Pol $\delta$  mispair generation can act differentially at different sites during replication of the two DNA strands.

In the DBY747 *pol3-L612M msh2* strain, the orientation dependence of site specific hot spots is greatly diminished, regardless of whether *URA3* was 1.2 or 10 kb away from ARS306. In fact, all the hot spots in *URA3* were observed at various rates in both OR1 and OR2 (Figures 3 and 4). When *URA3* was integrated ~600 bp from ARS1, the only hotspot exhibiting strong orientation dependence was C310T (Figure 5). Thus, in the DBY747 strain, the overall rates of Pol3-L612M dependent signatures in the MMR deficient background were nearly equal in the leading and lagging strands. This would suggest that in this strain background, Pol  $\delta$  generated mispairs are recognized and removed by MMR from both strands with equal efficiency, unlike that seen in the S288C background.

In summary, our finding that in both the S288C and DBY747 strains carrying the *pol3-L612M msh2* mutations, L612M Pol $\delta$  generated errors occur on both the leading and the lagging DNA strands, strongly suggests that Pol $\delta$  plays a major role in replicating both strands. Furthermore, they indicate that mismatch removal processes can act differentially in different yeast strains.

### Absence of Pole Signature Mutations in *pol2-M644G msh2*

Our conclusion that Pol $\delta$  replicates both DNA strands required a re-evaluation of the proposal that Pol $\epsilon$  replicates the leading strand (Pursell et al., 2007). This inference was based on the mutational bias for T:dTMP mispair formation on the leading strand in the *pol2-M644G* strain (Pursell et al., 2007). A major role of Pol $\epsilon$  in leading strand replication posits that the prevalence of Pol $\epsilon$  signature mutations on the leading strand would be greatly elevated in the absence of mismatch removal processes, since Pol $\epsilon$ -generated errors would not be removed. However, the complete absence of hot spot mutations in the S288C strain carrying the *pol2-M644G msh2* mutations indicates that the signature mutations that were

assigned to Polε's role in leading strand replication actually occur at a very low rate. Furthermore, in the *pol2-M644G msh2* strain, even the non-hot spot signature A-T and reciprocal T-A mutations are rare and do not exhibit leading strand preference. In fact, in the OR2 orientation, which exhibited extensive bias in the *pol2-M644G* single mutant, we find a 2:1 bias for T:dTTP mispair formation in the lagging strand in the *pol2-M644G msh2* mutant (Figure 6).

The absence of M644G Polε signature mutations on the leading strand has also been reported for the I(-2)I-7B-YUNI300 strain harboring the *pol2-M644G msh2* mutations (Lujan et al., 2012). Among the ~600 total *ura3* mutants sequenced for the two orientations, there was 1 A to T mutation on each of the DNA strands at A279, no A to T mutation on the leading strand at A686, and a total of only 3 and 2 A to T mutations were observed on the leading and lagging strands, respectively. Thus, even though M644G Polε exhibits an ~40-fold bias for the formation of T:dTTP mispair over the reciprocal A:dATP mispair, this mutation is almost completely absent in the mutational spectra of the *pol2-M644G msh2* strain. Thus, data in two different yeast strains support the conclusion that the DNA polymerase activity of Polε is not significantly involved in the replication of the leading strand as previously suggested from the analyses of mutational spectra in *pol2-M644G* alone (Pursell et al., 2007).

Furthermore, the *ura3* A279T and A686T hotspot mutations arise also in yeast harboring the *pol2-4* exonuclease mutant in an orientation dependent manner identical to that observed in the *pol2-M644G* mutant in the I(-2)I-7B-YUNI300 and S288C strain backgrounds [(Williams et al., 2012); our unpublished observations]. Thus, T:dTTP mispairs in the leading strand occur in the *pol2-4* mutant, in which there is no bias to generate this specific mispair, at rates similar to the *pol2-M644G* mutant strain in which there is a 40-fold bias for T:dTTP mispairs. These observations suggest that T:dTMP hot spot mispairs persist in the *pol2-4* or the *pol2-M644G* mutant strains because they are not removed by either the *pol2-4* or the *pol2-M644G* mutant polymerases (Ganai et al., 2015).

### Variability in Strand Specific Mismatch Correction Processes in Different Yeast Strains

In contrast to our observations indicating a prominent role of MMR in the correction of L612M Polδ errors in *URA3* on both the DNA strands in yeast strains S288C and DBY747, in the prior study in *msh2* cells, L612M Polδ-generated replication errors in the *URA3* gene were restricted to the lagging strand (Nick McElhinny et al., 2008). Subsequently, this observation was extended to the entire genome by deep sequencing analysis (Larrea et al., 2010). We note that all these other studies used the yeast strain I(-2)I-7B-YUNI300 which was derived from extensive crossings to mutator strains, including to a *pol3-01* mutator strain that is defective in Polδ 3'→5' proofreading exonuclease function (Pavlov et al., 2001) and to a *pol2-11* Polε mutant strain and to a DNA repair defective *rad5-G535R* strain (Figure S6); thus, this strain may harbor mutations that may have arisen during its derivation. By contrast, our studies utilized the more commonly used S288C and DBY747 yeast strains. S288C is the principal progenitor of most laboratory yeast strains (Mortimer and Johnston, 1986), and the complete genomic sequence of this strain has been determined.

Two different possibilities could account for the lack of L612M Pol $\delta$  signature mutations on the leading strand in the absence of MMR in the I(-2)I-7B-YUNI300 strain. The first possibility is that, unique to this yeast strain, Pol $\epsilon$  and Pol $\delta$  are restricted to replicating the leading strand and lagging strands, respectively. However, in this strain background, in spite of the very highly elevated bias of M644G Pol $\epsilon$  for T:dTTP mispair (~40-fold) over the reciprocal A:dATP mispair, there is complete absence of bias for M644G-Pol $\epsilon$  signature mutations on the leading strand in the *pol2 M644G msh2* strain (Lujan et al., 2012). Since the bias of mutant Pol $\epsilon$  for T:dTTP mispair exceeds the bias for any of the signature mutations made by mutant Pol $\delta$ , one would have expected to see a highly elevated level of Pol $\epsilon$  signature mutations on the leading strand in the *pol2 M644G msh2* strain. The absence of any bias for Pol $\epsilon$  signature mutations on the leading strand in the I(-2)I-7B-YUNI300 strain, as well as in the S288C strain, therefore is not consistent with the division of labor model of DNA replication. More likely is the second possibility that in the I(-2)I-7B-YUNI300 strain, as seen in the S288C and DBY747 strains, Pol $\delta$  replicates both DNA strands, and the lack of L612M Pol $\delta$  signature mutations on the leading strand in the absence of MMR is due to the more efficient removal of Pol $\delta$  generated errors by Pol $\epsilon$  exonuclease on the leading than on the lagging strand. Consequently, L612M-Pol $\delta$  signature errors would appear to be biased towards the lagging strand, even though the actual mismatch generation frequencies by Pol $\delta$  were similar on both strands. This explanation would also account for the L612M-Pol $\delta$  leading strand signature bias observed genome wide, as detected by deep sequencing.

### Ribonucleotide Incorporation in the *pol2-M644G Pol $\epsilon$* Mutant

In addition to T:dTTP mispair formation bias, the Pol $\epsilon$ -M644G enzyme exhibits a highly increased capacity for ribonucleotide incorporation in DNA (Lujan et al., 2013; Nick McElhinny et al., 2010). From the observation that in the absence of RNase H2, ribonucleotides persist in the nascent leading strand in the *pol2-M644G* mutant, it has been inferred that Pol $\epsilon$  replicates the leading strand (Lujan et al., 2013). However, it is difficult to reconcile this interpretation with our evidence that Pol $\delta$  participates equally in the replication of both the leading and lagging DNA strands, and with the lack of any evidence for a role of Pol $\epsilon$  in the replication of the leading strand as deduced from the absence of Pol $\epsilon$  signature mutations in the *pol2-M644G msh2* strain. This raises the possibility that an explanation other than a role of Pol $\epsilon$  in the replication of the leading strand accounts for the increased presence of rNMPs in the nascent leading strand in the M644G Pol $\epsilon$  mutant.

The Pol $\delta$  3'→5' exonuclease lacks the ability to proofread rNMPs (Clausen et al., 2013); however, since Pol $\epsilon$  exonuclease can excise them (Williams et al., 2012), it would play an important role in their removal from the leading strand. We suggest that in yeast harboring the M644G Pol $\epsilon$  mutation, because of the reduction in its proofreading activity (Ganai et al., 2015) and because of its highly elevated propensity to extend synthesis from rNMPs incorporated into the nascent leading strand by Pol $\delta$  (Lujan et al., 2013), the mutant Pol $\epsilon$  promotes the persistence of rNMPs in the leading strand. Consequently, increased rNMP levels in the nascent leading strand in the *pol2-M644G* mutant in the absence of RNase H2 would not arise from a role of Pol $\epsilon$  as the major leading strand replicase, but rather from a

lack of their removal and from the highly proficient extension of synthesis from rNMPs misincorporated by Pol $\delta$ .

### Roles of Pol $\delta$ and Pole in DNA Replication in *S. pombe*

From studies with *S. pombe* harboring *Pol $\delta$ -L591M* and *Pole-M630F* mutations, it was concluded that Pol $\delta$  replicates the lagging strand and that Pole replicates the leading strand in fission yeast also. For this study, the mutational spectra of a *ura4/ura5* cassette, in two orientations near an active ARS, was analyzed in the *Pol $\delta$ -L591M* mutant. Mutations were scattered throughout the coding region, and localized hotspots were not observed. However, from the numbers of T:A $\rightarrow$ C:G and G:C $\rightarrow$ A:T mutations, predicted to derive from the T:dG and G:dT mispairs, respectively, a role for Pol $\delta$  in the replication of the lagging strand was inferred (Miyabe et al., 2011). Notably, mutational changes which indicated an elevated bias of Pol $\delta$  for mispair formation on the leading strand were not considered. In Figure S7, we plot the data provided in their Table 2 (Miyabe et al., 2011) calculated as the percentages of each type of signature mutation apportioned to either leading or lagging strand based upon the bias for mispair formation determined for the *S. cerevisiae* L612M Pol $\delta$  enzyme (Table S6). Although there is a bias for the formation of G:dT (~2-fold) and T:dG (~3-8 fold) mispairs on the lagging strand, for the other signature mutations, there is either no bias on the lagging strand, or there is evidence for biased mispair formation on the leading strand (Table S6, Figure S7). In particular, for example, are the data for the G:dA mispair, which is formed by mutant Pol $\delta$  with an 8.5--fold elevated bias over the reciprocal C:dT mispair (see Figure 2A). In the reverse orientation where there is a high prevalence of G to T mutations, there is an ~ 5 fold bias for the G:dA mispair on the leading strand over the lagging strand (Table S6, Figure S7). Frameshift mutations also suggest the presence of mutant Pol $\delta$  dependent mutations on both DNA strands. For example, despite an 11-fold and 17-fold bias of mutant L612M Pol $\delta$  in the formation of T and G over A and C, respectively (Nick McElhinny et al., 2007), in the in the reverse orientation, these mutations occur in both strands at similar rates. In the forward orientation, however, there is ~2 fold bias for T in the lagging strand, but a 9 fold bias for G mutations formed in the leading strand (Table S6 and Figure S7). Based on the presumption that Pol $\delta$  synthesizes both strands in *S. pombe*, the total Pol $\delta$  signature mutations on both strands should be nearly equal. As calculated from their data, overall, the Pol $\delta$  signature mutations on the leading strand in the reverse orientation are slightly higher than on the lagging strand, and in the forward orientation they are only 2-fold higher on the lagging strand than on the leading strand. Thus, altogether, rather than providing definitive evidence for the involvement of pol $\delta$  in the replication of only the lagging strand, their data (Miyabe et al., 2011) support a role of Pol $\delta$  in the replication of both the leading and lagging DNA strands in *S. pombe*.

Furthermore, their analysis of the *ura4-ura5* mutation bias in *pole-M630F* and *pole-M630F msh2* mutants failed to provide any evidence of a bias for Pole signature mutations on the leading strand in *S. pombe* (Miyabe et al., 2011). Nevertheless, a role for Pole in the replication of the leading strand was inferred from the evidence of increased rNMP incorporation in the nascent leading strand in the absence of RNase H2 in the *S. pombe pole-M630F* mutant (Miyabe et al., 2011). However, in view of the evidence indicating the presence of signature mutations on both the DNA strands in the *pol $\delta$ -L591M* strain (Table

S6, Figure S7), and the absence of Pol $\epsilon$  signature mutations in the *pol\epsilon-M630F msh2* double mutant, it is difficult to assign a role for Pol $\epsilon$  in the replication of the leading strand based on the observation of increased rNMP incorporation in the *Pol\epsilon-M630F* mutant. That is because in *S. pombe* also, increased presence of rNMPs on the nascent leading strand in the *pol\epsilon-M630F* mutant would result from the propensity of mutant Pol $\epsilon$  to extend synthesis from rNMPs incorporated by Pol $\delta$  on the leading strand, and not from its role as a major replicase for the leading strand.

Recently, the genome wide incorporation of rNMPs in the two DNA strands has been reported for the Pol $\epsilon$  and Pol $\delta$  mutants of *S. cerevisiae* and *S. pombe* (Clausen et al., 2015; Daigaku et al., 2015; Koh et al., 2015; Reijns et al., 2015). Similar to previously reported observations (Lujan et al., 2013; Miyabe et al., 2011), these studies indicate a leading strand bias for rNMP incorporation by mutant Pol $\epsilon$ . As discussed above, these observations can all be explained by the reduced efficiency of mutant Pol $\epsilon$  for rNMP removal and by its greatly enhanced proficiency for extending synthesis from rNMPs.

### Roles of Pole on the Leading Strand

In both the budding yeast and the fission yeast, the N-terminal polymerase domain of the catalytic subunit of Pol $\epsilon$  is not required for cell viability, whereas the C-terminal domain (CTD) is essential (Feng and D'Urso, 2001; Kesti et al., 1999). The essential role of Pol $\epsilon$  CTD, but not the polymerase domain, has also been observed for DNA replication in the *Drosophila* imaginal eye disks (Suyari et al., 2012). Elegant genetic studies with a temperature-sensitive mutation in the CTD of the catalytic subunit of Pol $\epsilon$  (*cdc20-ct1*) in *S. pombe* have shown that Pol $\epsilon$  plays an essential role in both the assembly and progression of CMG helicase (Handa et al., 2012), which unwinds the DNA duplex by translocating along the leading strand in a 3'  $\rightarrow$  5' direction (Fu et al., 2011; Ilves et al., 2010; Moyer et al., 2006). Since the C-terminal domain of the catalytic subunit of Pol $\epsilon$  lacks the DNA polymerase function, the DNA polymerization activity of Pol $\epsilon$  is not required for this essential role.

Recently, the association of replication proteins with the leading and lagging strands of DNA replication forks has been analyzed in yeast using the eSPAN (enrichment and sequencing of protein-associated nascent DNA) method (Yu et al., 2014). Their observations that Pol $\epsilon$  and Pol $\delta$  associate preferentially with the leading and lagging DNA strands, respectively, are consistent with the role of Pol $\delta$  in replicating both strands and with the role of Pol $\epsilon$  in the progression of CMG complex on the leading strand. The density of Pol $\delta$  would be much higher on the lagging strand because it is synthesized in a discontinuous manner, and Pol $\epsilon$  would be restricted primarily to the leading strand because of its CMG associated role. In other recently reported biochemical reconstitution studies, from the observation that Pol $\epsilon$  binds tightly to the CMG complex and carries out highly efficient synthesis of the leading strand, it has been inferred that the CMG complex recruits Pol $\epsilon$  for leading strand synthesis (Georgescu et al., 2014; Langston et al., 2014). However, our genetic studies indicating the requirement of Pol $\delta$ , but not of Pol $\epsilon$ , for leading strand replication, imply that *in vivo*, only the non-catalytic role of Pol $\epsilon$  in the assembly and progression of the CMG complex is utilized for leading strand replication.

The placement of Pol $\epsilon$  with CMG on the leading strand would enable Pol $\epsilon$  to function in diverse roles on this DNA strand. Thus, Pol $\epsilon$  exonuclease could play a more prominent role in the correction of replication errors generated by Pol $\delta$  on the leading strand than on the lagging strand. Furthermore, since Pol $\delta$  exonuclease lacks the ability to proofread rNMPs, but Pol $\epsilon$  exonuclease has this ability, rNMPs incorporated during replication of the leading strand by Pol $\delta$  would be subject to removal by Pol $\epsilon$  exonuclease. The placement of Pol $\epsilon$  on the leading strand would also allow Pol $\epsilon$  to function as an accessory polymerase, substituting for Pol $\delta$  in situations where its ability to carry out replication is compromised. For example, Pol $\epsilon$  could take over synthesis at sites where Pol $\delta$  replication stalls, and Pol $\epsilon$  could play an important role in the repair of the leading strand, e.g., at nicks in the template strand, Pol $\epsilon$  could mediate the repair of strand breaks in coordination with S phase checkpoint (Navas et al., 1995; Sukhanova et al., 2011).

### Concluding remarks

The major findings of this study and their implications are summarized below.

- (1) Our observations indicating the prevalence of L612M Pol $\delta$  generated signature mutations on both the DNA strands in *pol3-L612M msh2* at different positions in the genome in two different *S. cerevisiae* strains provide positive proof for the conclusion that Pol $\delta$  replicates both the leading and lagging DNA strands.
- (2) In agreement with the role of Pol $\delta$  in the replication of both DNA strands, genetic analyses with the *pol2-M644G* Pol $\epsilon$  mutant lacking MMR have failed to provide any evidence for the involvement of Pol $\epsilon$  in the synthesis of the leading strand.
- (3) We provide evidence that in addition to MMR, Pol $\epsilon$  exonuclease and Exo1 function in the removal of Pol $\delta$  replication errors from the two DNA strands, and that these different mismatch removal processes can act differentially on the leading and lagging DNA strands. We suggest that yeast strains differ in the relative contributions of different mismatch removal processes for correcting Pol $\delta$  errors from the two DNA strands.
- (4) Previously, it was concluded that in *S. pombe*, Pol $\delta$  and Pol $\epsilon$  replicate the lagging and leading strands, respectively. A reconsideration of published data, however, implicates a role of Pol $\delta$  in the replication of both the leading and lagging DNA strands in *S. pombe* also.

## EXPERIMENTAL PROCEDURES

### Determination of Spontaneous Reversion Rates and Mutational Changes at *ura3-104*

For each strain, 11 independent cultures, each starting from ~50 cells were grown in 15 ml of YPD medium, washed with water and plated on SC-ura media. Cell viability was determined from the number of colonies formed on SC media plated from serial dilutions of the original culture. Rates of *ura3-104* reversion were determined from the number of Ura<sup>+</sup> colonies by the method of the median (Lea and Coulson, 1949). Five experiments were performed with each strain. For sequence determination, a large number of independent

cultures were grown and plated on SC-ura media. One Ura<sup>+</sup> colony from each independent culture was subcloned on medium lacking uracil and subsequently patched onto yeast extract-peptone-dextrose (YPD) medium. Genomic DNA was isolated from patches and the *URA3* gene amplified via PCR using oligos LP2221 (5'-GCCCAGTATTCTTAACCCA-3') and LP2222 (5'-GTGAGTTTAGTATACATGC-3'). Mutations at the *ura3-104* amber codon were then identified by DNA sequencing with oligo LP2221.

### ***URA3* to *ura3* Mutation Rates and Mutational Spectra**

Spontaneous forward mutation rates of *URA3* in OR1 and OR2 were determined using the method of the median as described above. For each strain, 15 independent cultures, each starting from ~50 cells were grown in 0.2 to 3 ml of YPD medium and grown for 3 days. Cells were washed and resuspended in sterile water before plating on synthetic complete (SC) media containing 5-FOA for the S288C strains and on SC-trp media containing 5-FOA for the DBY747 strains. Cell viability was determined as above. For sequence analyses, a large number of independent cultures were grown, washed, and plated on media as described above. A single FOA<sup>r</sup> colony from each culture was patched onto YPD. Genomic DNA was extracted, and the *ura3* gene was amplified via PCR as above and PCR products were sequenced using oligos LP2221 and LP2222.

### **Protein Purification and DNA Synthesis Assays**

The *pol3 L612M* mutant protein which was proficient in its proofreading exonuclease or deficient in it was expressed from a *GAL:PGK* promoter, and the wild type and mutant Pol3 proteins were purified by glutathione sepharose as described (Swan et al., 2009). The wild type and L612M mutant Pol $\delta$  holoenzymes which were proficient in proofreading exonuclease were purified as described (Acharya et al., 2011). DNA synthesis assays were performed at 30°C (Acharya et al., 2011) under conditions indicated in the legend to Figure S2.

### **Supplementary Material**

Refer to Web version on PubMed Central for supplementary material.

### **ACKNOWLEDGMENTS**

This work was supported from a grant, CA107650, from the National Institutes of Health.

### **REFERENCES**

- Acharya N, Klassen R, Johnson RE, Prakash L, Prakash S. PCNA binding domains in all three subunits of yeast DNA polymerase delta modulate its function in DNA replication. *Proc. Natl. Acad. Sci. USA.* 2011; 108:17927–17932. [PubMed: 22003126]
- Boulet A, Simon M, Faye G, Gauer GA, Burgers PMJ. Structure and function of the *Saccharomyces cerevisiae CDC2* gene encoding the large subunit of DNA polymerase III. *EMBO J.* 1989; 8:1849–1854. [PubMed: 2670563]
- Clausen AR, Lujan SA, Burkholder AB, Orebaugh CD, Williams JS, Clausen MF, Malc EP, Mieczkowski PA, Fargo DC, Smith DJ, et al. Tracking replication enzymology in vivo by genome-wide mapping of ribonucleotide incorporation. *Nat. Struct. Mol. Biol.* 2015



- Clausen AR, Zhang S, Burgers PM, Lee MY, Kunkel TA. Ribonucleotide incorporation, proofreading and bypass by human DNA polymerase delta. *DNA Repair (Amst)*. 2013; 12:121–127. [PubMed: 23245697]
- Daigaku Y, Keszthelyi A, Muller CA, Miyabe I, Brooks T, Retkute R, Hubank M, Nieduszynski CA, Carr AM. A global profile of replicative polymerase usage. *Nat. Struct. Mol. Biol.* 2015
- Feng W, D'Urso G. *Schizosaccharomyces pombe* cells lacking the amino-terminal catalytic domains of DNA polymerase epsilon are viable but require the DNA damage checkpoint control. *Mol. Cell. Biol.* 2001; 21:4495–4504. [PubMed: 11416129]
- Fu YV, Yardimci H, Long DT, Ho TV, Guainazzi A, Bermudez VP, Hurwitz J, van Oijen A, Scharer OD, Walter JC. Selective bypass of a lagging strand roadblock by the eukaryotic replicative DNA helicase. *Cell*. 2011; 146:931–941. [PubMed: 21925316]
- Ganai RA, Bylund GO, Johansson E. Switching between polymerase and exonuclease sites in DNA polymerase  $\epsilon$ . *Nucleic Acids Res.* 2015; 43:932–942. [PubMed: 25550436]
- Genschel J, Bazemore LR, Modrich P. Human exonuclease I is required for 5' and 3' mismatch repair. *J. Biol. Chem.* 2002; 277:13302–13311. [PubMed: 11809771]
- Georgescu RE, Langston L, Yao NY, Yurieva O, Zhang D, Finkelstein J, Agarwal T, O'Donnell ME. Mechanism of asymmetric polymerase assembly at the eukaryotic replication fork. *Nat Struct Mol Biol.* 2014; 21:664–670. [PubMed: 24997598]
- Handa T, Kanke M, Takahashi TS, Nakagawa T, Masukata H. DNA polymerization-independent functions of DNA polymerase epsilon in assembly and progression of the replisome in fission yeast. *Molecular biology of the cell*. 2012; 23:3240–3253. [PubMed: 22718908]
- Hartwell LH. Sequential function of gene products relative to DNA synthesis in the yeast cell cycle. *J. Mol. Biol.* 1976; 104:803–817. [PubMed: 785015]
- Ilves I, Petojevic T, Pesavento JJ, Botchan MR. Activation of the MCM2-7 helicase by association with Cdc45 and GINS proteins. *Mol. Cell*. 2010; 37:247–258. [PubMed: 20122406]
- Johnson RE, Kovvali GK, Prakash L, Prakash S. Requirement of the yeast *MSH3* and *MSH6* genes for *MSH2*-dependent genomic stability. *J. Biol. Chem.* 1996; 271:7285–7288. [PubMed: 8631743]
- Kesti T, Flick K, Keranen S, Syvaaja JE, Wittenberg C. DNA polymerase  $\epsilon$  catalytic domains are dispensable for DNA replication, DNA repair, and cell viability. *Mol. Cell*. 1999; 3:679–685. [PubMed: 10360184]
- Koh KD, Balachander S, Hesselberth JR, Storic F. Ribose-seq: global mapping of ribonucleotides embedded in genomic DNA. *Nat. Methods*. 2015; 12:251–257. [PubMed: 25622106]
- Langston LD, Zhang D, Yurieva O, Georgescu RE, Finkelstein J, Yao NY, Indiani C, O'Donnell ME. CMG helicase and DNA polymerase epsilon form a functional 15-subunit holoenzyme for eukaryotic leading-strand DNA replication. *Proc. Natl. Acad. Sci. USA*. 2014; 111:15390–15395. [PubMed: 25313033]
- Larrea AA, Lujan SA, Nick McElhinny SA, Mieczkowski PA, Resnick MA, Gordenin DA, Kunkel TA. Genome-wide model for the normal eukaryotic DNA replication fork. *Proc. Natl. Acad. Sci. USA*. 2010; 107:17674–17679. [PubMed: 20876092]
- Lea DE, Coulson CA. The distribution of the numbers of mutants in bacterial populations. *Journal of Genetics*. 1949; 49:264–285. [PubMed: 24536673]
- Lujan SA, Williams JS, Clausen AR, Clark AB, Kunkel TA. Ribonucleotides are signals for mismatch repair of leading-strand replication errors. *Mol. Cell*. 2013; 50:437–443. [PubMed: 23603118]
- Lujan SA, Williams JS, Pursell ZF, Abdulovic-Cui AA, Clark AB, Nick McElhinny SA, Kunkel TA. Mismatch repair balances leading and lagging strand DNA replication fidelity. *PLoS Genet*. 2012; 8:e1003016. [PubMed: 23071460]
- Miyabe I, Kunkel TA, Carr AM. The major roles of DNA polymerases epsilon and delta at the eukaryotic replication fork are evolutionarily conserved. *PLoS Genet*. 2011; 7:e1002407. [PubMed: 22144917]
- Morrison A, Bell JB, Kunkel TA, Sugino A. Eukaryotic DNA polymerase amino acid sequence required for 3'----5' exonuclease activity. *Proc. Natl. Acad. Sci. USA*. 1991; 88:9473–9477. [PubMed: 1658784]
- Mortimer RK, Johnston JR. Genealogy of principal strains of the yeast genetic stock center. *Genetics*. 1986; 113:35–43. [PubMed: 3519363]

- Moyer SE, Lewis PW, Botchan MR. Isolation of the Cdc45/Mcm2-7/GINS (CMG) complex, a candidate for the eukaryotic DNA replication fork helicase. *Proc. Natl. Acad. Sci. USA.* 2006; 103:10236–10241. [PubMed: 16798881]
- Navas TA, Zhou Z, Elledge SJ. DNA polymerase epsilon links the DNA replication machinery to the S phase checkpoint. *Cell.* 1995; 80:29–39. [PubMed: 7813016]
- Nick McElhinny SA, Gordenin DA, Stith CM, Burgers PMJ, Kunkel TA. Division of labor at the eukaryotic replication fork. *Mol. Cell.* 2008; 30:137–144. [PubMed: 18439893]
- Nick McElhinny SA, Kumar D, Clark AB, Watt DL, Watts BE, Lundstrom EB, Johansson E, Chabes A, Kunkel TA. Genome instability due to ribonucleotide incorporation into DNA. *Nat Chem Biol.* 2010; 6:774–781. [PubMed: 20729855]
- Nick McElhinny SA, Stith CM, Burgers PM, Kunkel TA. Inefficient proofreading and biased error rates during inaccurate DNA synthesis by a mutant derivative of *Saccharomyces cerevisiae* DNA polymerase delta. *J. Biol. Chem.* 2007; 282:2324–2332. [PubMed: 17121822]
- Nieduszynski CA, Hiraga S, Ak P, Benham CJ, Donaldson AD. OriDB: a DNA replication origin database. *Nucleic Acids Res.* 2007; 35:D40–46. [PubMed: 17065467]
- Pavlov YI, Shcherbakova PV, Kunkel TA. In vivo consequences of putative active site mutations in yeast DNA polymerases alpha, epsilon, delta, and zeta. *Genetics.* 2001; 159:47–64. [PubMed: 11560886]
- Pursell ZF, Isoz I, Lundstrom E-B, Johansson E, Kunkel TA. Yeast DNA polymerase  $\epsilon$  participates in leading-strand DNA replication. *Science.* 2007; 317:127–130. [PubMed: 17615360]
- Reijns MA, Kemp H, Ding J, de Proce SM, Jackson AP, Taylor MS. Lagging-strand replication shapes the mutational landscape of the genome. *Nature.* 2015; 518:502–506. [PubMed: 25624100]
- Simon M, Giot L, Faye G. The 3' to 5' exonuclease activity located in the DNA polymerase  $\delta$  subunit of *Saccharomyces cerevisiae* is required for accurate replication. *EMBO J.* 1991; 10:2165–2170. [PubMed: 1648480]
- Sitney KC, Budd ME, Campbell JE. DNA polymerase III, a second essential DNA polymerase, is encoded by the *S. cerevisiae CDC2* gene. *Cell.* 1989; 56:599–605. [PubMed: 2645055]
- Sokolsky T, Alani E. EXO1 and MSH6 are high-copy suppressors of conditional mutations in the MSH2 mismatch repair gene of *Saccharomyces cerevisiae*. *Genetics.* 2000; 155:589–599. [PubMed: 10835383]
- Sukhanova MV, D'Herin C, van der Kemp PA, Koval VV, Boiteux S, Lavrik OI. Ddc1 checkpoint protein and DNA polymerase epsilon interact with nick-containing DNA repair intermediate in cell free extracts of *Saccharomyces cerevisiae*. *DNA Repair (Amst).* 2011; 10:815–825. [PubMed: 21601535]
- Suyari O, Kawai M, Ida H, Sakaguchi K, Yamaguchi M. Differential requirement for the N-terminal catalytic domain of the DNA polymerase  $\epsilon$  p255 subunit in the mitotic cell cycle and the endocycle. *Gene.* 2012; 495:104–114. [PubMed: 22245183]
- Swan MK, Johnson RE, Prakash L, Prakash S, Aggarwal AK. Structural basis of high-fidelity DNA synthesis by yeast DNA polymerase  $\delta$ . *Nat. Struct. Mol. Biol.* 2009; 16:979–986. [PubMed: 19718023]
- Tishkoff DX, Boerger AL, Bertrand P, Filosi N, Gaida GM, Kane MF, Kolodner RD. Identification and characterization of *Saccharomyces cerevisiae EXO1*, a gene encoding an exonuclease that interacts with MSH2. *Proc. Natl. Acad. Sci. USA.* 1997; 94:7487–7492. [PubMed: 9207118]
- Tran HT, Gordenin DA, Resnick MA. The 3'  $\rightarrow$  5' exonucleases of DNA polymerase  $\delta$  and  $\epsilon$  and the 5'  $\rightarrow$  3' exonuclease Exo1 have major roles in postreplication mutation avoidance in *Saccharomyces cerevisiae*. *Mol. Cell. Biol.* 1999; 19:2000–2007. [PubMed: 10022887]
- Tsurimoto, Stillman B. Replication factors required for SV40 DNA replication *in vitro*. II. Switching of DNA polymerase alpha and delta during initiation of leading and lagging strand synthesis. *J. Biol. Chem.* 1991a; 266:1961–1968. [PubMed: 1671046]
- Tsurimoto T, Melendy T, Stillman B. Sequential initiation of lagging and leading strand synthesis by two different polymerase complexes at the SV40 DNA replication origin. *Nature.* 1990; 346:534–539. [PubMed: 2165567]

- Tsurimoto T, Stillman B. Replication factors required for SV40 DNA replication *in vitro*. I. DNA structure-specific recognition of a primer-template junction by eukaryotic DNA polymerases and their accessory proteins. *J. Biol. Chem.* 1991b; 266:1950–1960. [PubMed: 1671045]
- Waga S, Stillman B. Anatomy of a DNA replication fork revealed by reconstitution of SV40 DNA replication *in vitro*. *Nature.* 1994; 369:207–212. [PubMed: 7910375]
- Williams JS, Clausen AR, Nick McElhinny SA, Watts BE, Johansson E, Kunkel TA. Proofreading of ribonucleotides inserted into DNA by yeast DNA polymerase  $\epsilon$ . *DNA Repair (Amst).* 2012; 11:649–656. [PubMed: 22682724]
- Yu C, Gan H, Han J, Zhou ZX, Jia S, Chabes A, Farrugia G, Ordog T, Zhang Z. Strand-specific analysis shows protein binding at replication forks and PCNA unloading from lagging strands when forks stall. *Mol Cell.* 2014; 56:551–563. [PubMed: 25449133]

### Highlights

- Pol $\delta$  generated errors occur on both the leading and lagging DNA strands
- Pol $\delta$  errors are removed by mismatch repair, Pole exonuclease, and Exo1
- Pol $\delta$  replicates both the leading and lagging DNA strands
- Pole does not replicate the leading strand

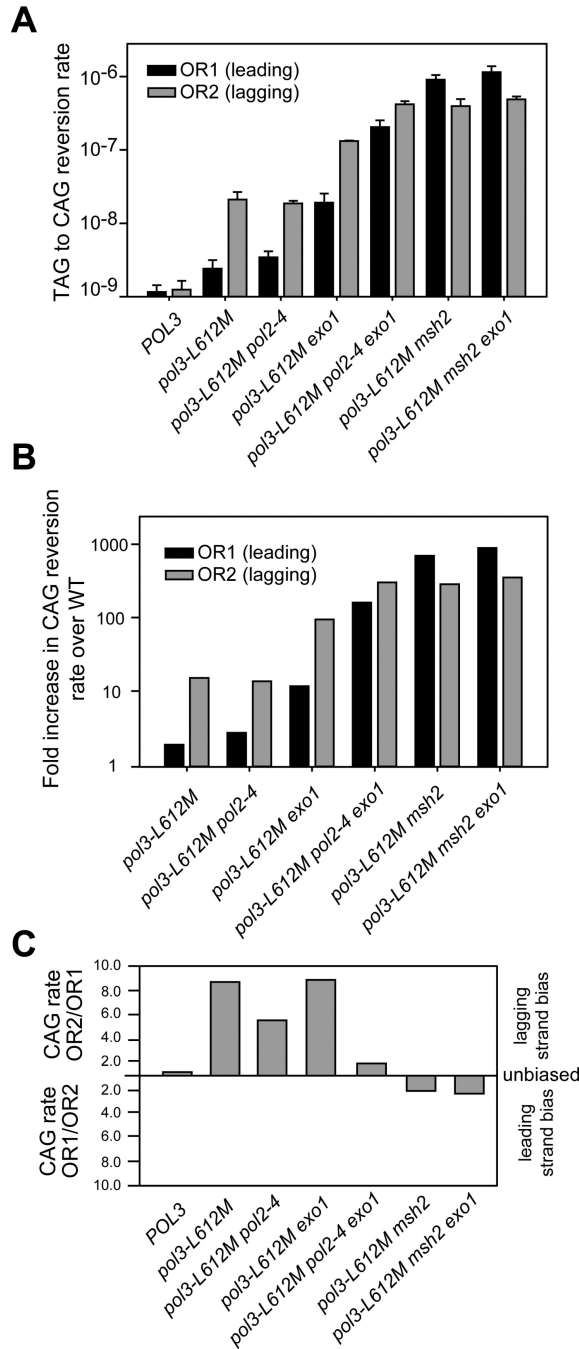


**Figure 1. Orientation bias of *ura3-104* reversion in the S288C *pol3-L612M* strains defective in Polε proofreading (*pol2-4*), MMR (*msh2*) or Exo1 (*exo1*)**  
 (A) CAG-specific reversion rates of *ura3-104* for various strains in orientations OR1 and OR2. (B) Fold increase in CAG-specific reversion rates in either OR1 or OR2. (C) Reversal of strand bias in Pol3-L612M mutation generation from lagging to leading strand by inactivation of mismatch removal processes.  
 See also Figures S1-S5.

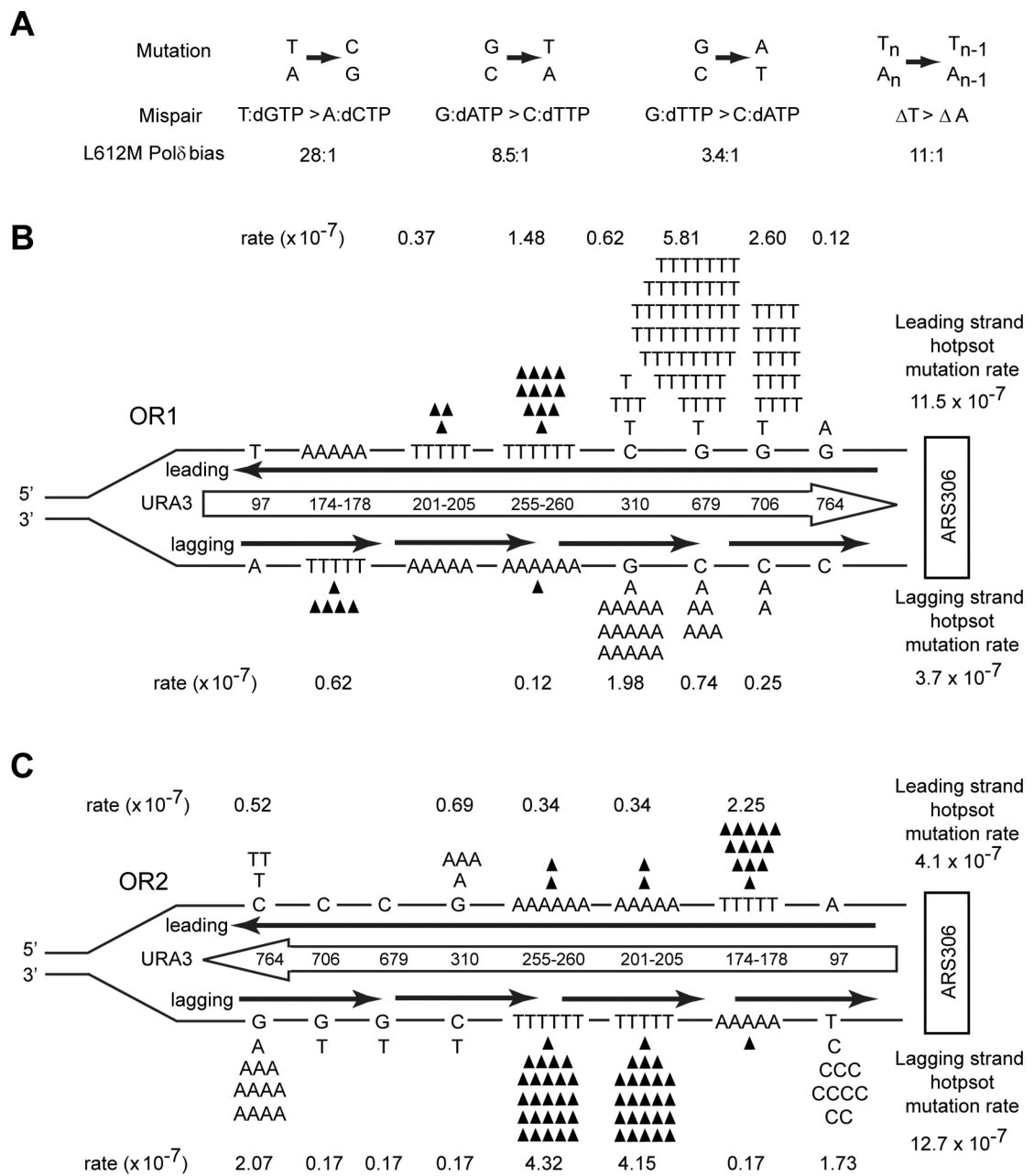


**Figure 2. Lack of strand bias of *URA3* mutations near *ARS306* in the S288C *pol3-L612M msh2* strain**

(A) Mismatch generation bias of L612M Pol $\delta$ . Point mutations are shown above the two mismatches that generate the mutation. The bias of L612M Pol $\delta$  for each mismatch is given below (Nick McElhinney, 2007) (B) Hot spot mutations in *URA3* observed in OR1 in the S288C *pol3-L612M msh2* strain. The orientation of the *URA3* ORF (boxed arrow) is depicted by the direction of the arrow. *URA3*, integrated ~1.2 kb to the left of *ARS306* in chromosome 3 is shown schematically and is not drawn to scale. Each hot spot is shown by their respective base pairs, and their positions in the *URA3* ORF are shown within the boxed arrow. Base changes generated during the replication of the leading strand (above) and the lagging strand

(below) are shown. Filled in triangles represent  $-1$  frameshift mutations. The proportion of observed mutations at each site were assigned to the lagging and leading strand according to the bias for mispair formation by L612M Pol $\delta$  shown in (A). Strand specific mutation rates for each site were calculated as described in the text, and the leading and lagging strand hot spot mutation rates given on the far right are the sum of all hot spot mutations on that strand. (C) Hot spot mutations in *URA3* observed in OR2 in the *pol3-L612M msh2* strain. The orientation of *URA3* is reversed from that in (B). See also Figures S2, S4, S5, and Tables S1 and S2.

Author Manuscript

Author Manuscript

Author Manuscript

Author Manuscript

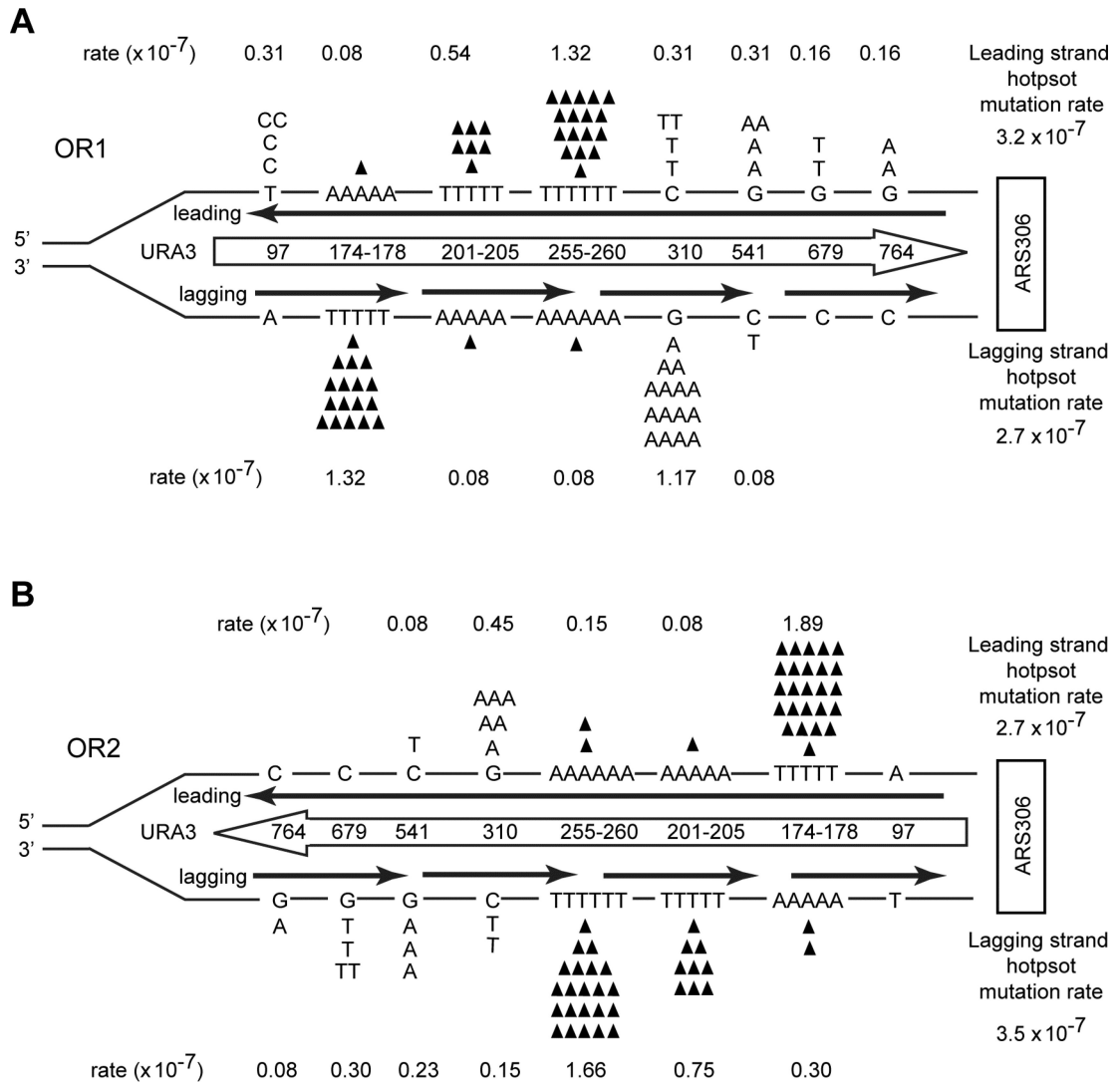


**Figure 3. Lack of strand bias of *URA3* mutations located near *ARS306* in the *DBY747 pol3-L612M msh2* strain**

(A) Hot spot mutations in *URA3* observed in OR1 in the *DBY747 pol3-L612M msh2* strain. The *URA3* coding region is integrated ~ 1.2 kb to the left of *ARS306* on chromosome 3 as described in Figure 2. (B) Hot spot mutations in *URA3* near *ARS306* observed in OR2 in the *pol3-L612M msh2* strain. The orientation of *URA3* is reversed from that in (A). The sum of all hotspot mutations for the leading or the lagging DNA strand is given on the right. See also Figure S4 and Table S3.



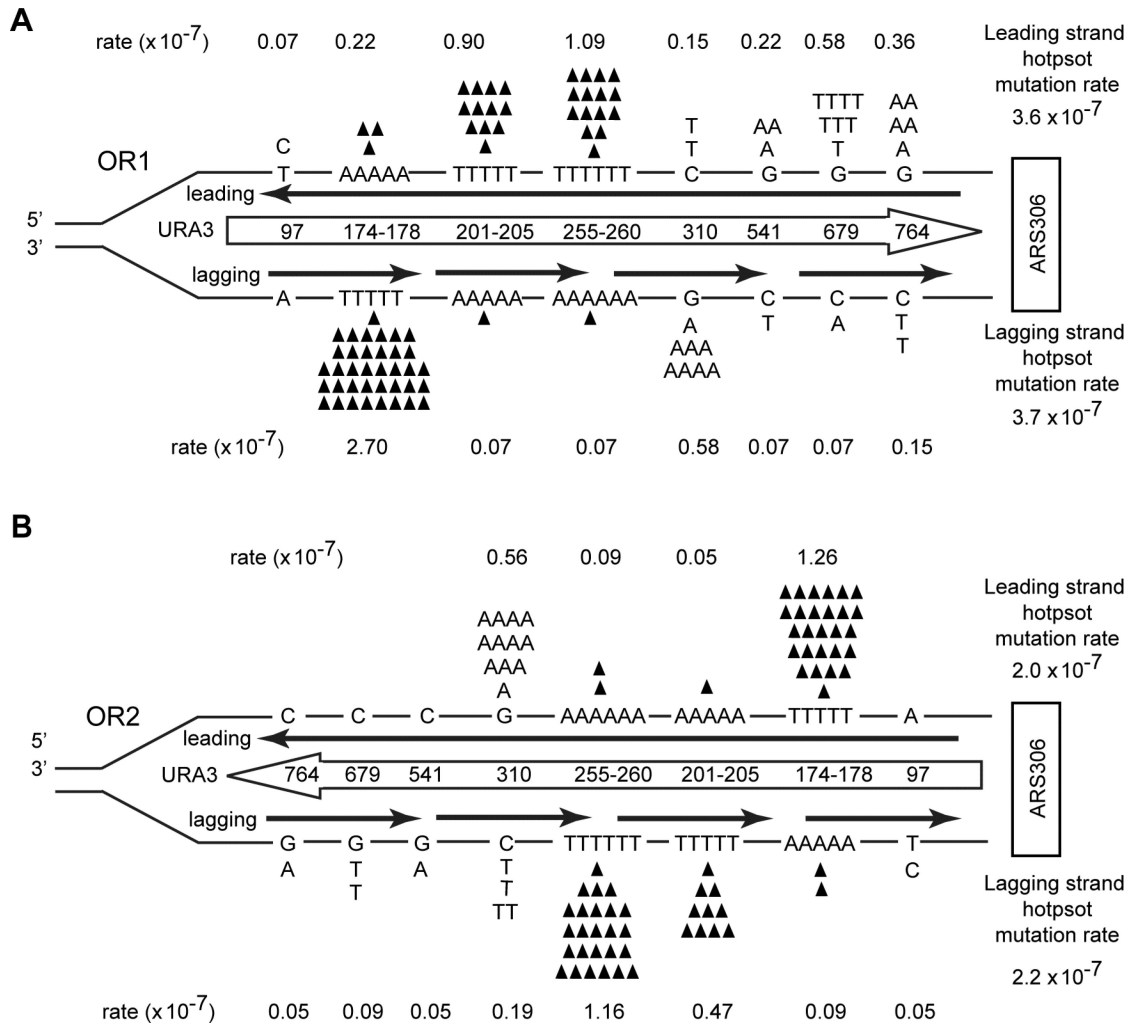


**Figure 4. Lack of strand bias of *URA3* mutations located ~10kb left of ARS306 in the DBY747 *pol3-L612M msh2* strain**

(A) Hot spot mutations in *URA3* observed in OR1 in the DBY747 *pol3-L612M msh2* strain. The *URA3* ORF (boxed arrow) is integrated ~10 kb to the left of ARS306 on chromosome 3 in the intergenic region between the *STE50* and *RRP1* genes. (B) Hot spot mutations observed in *URA3* located ~10 kb to the left of ARS306 in OR2 in the DBY747 *pol3-L612M msh2* strain. The orientation of *URA3* is reversed from that in (A). The sum of all hotspot mutations for the leading or the lagging DNA strand is given on the right. See also Table S4.

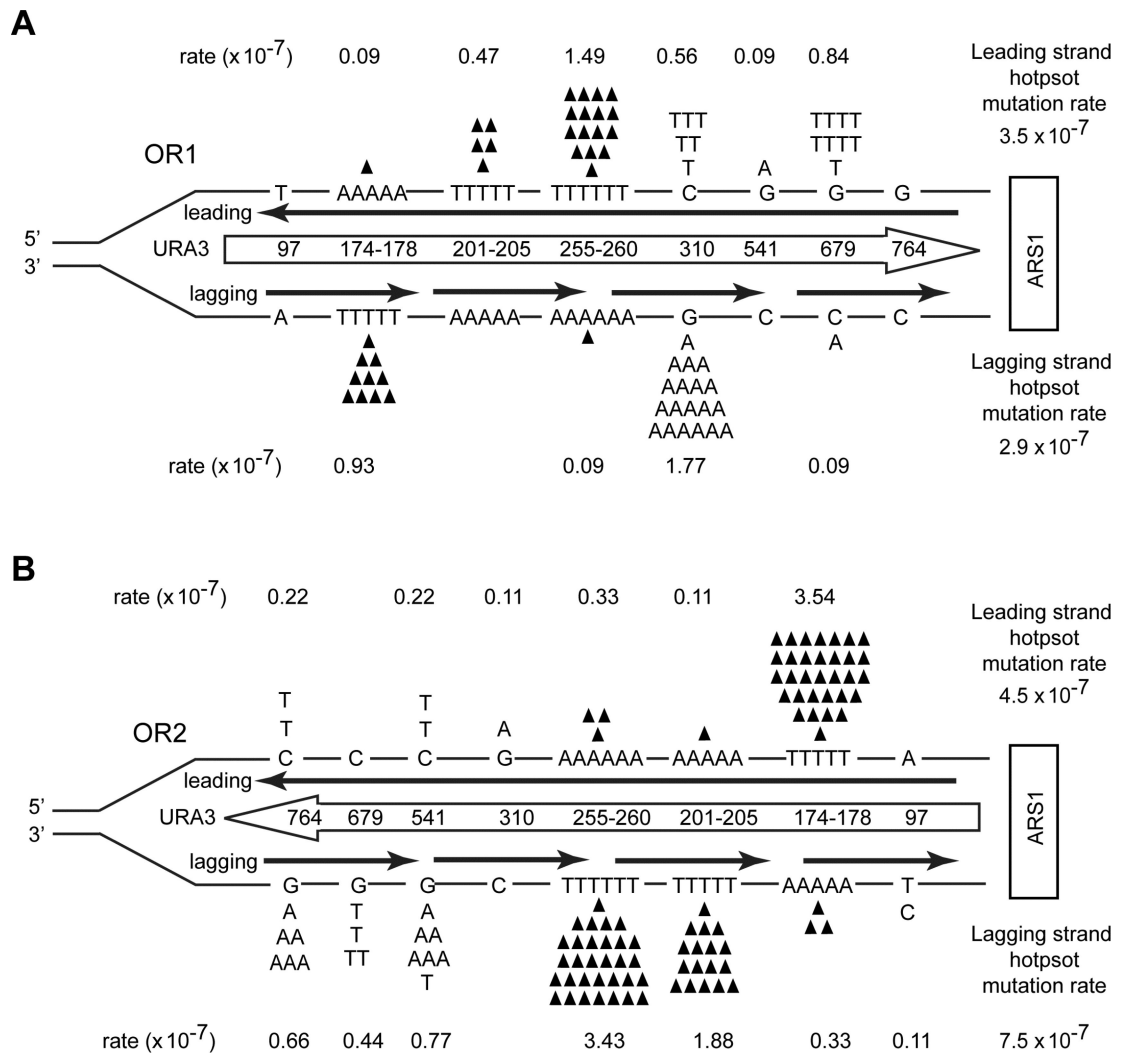


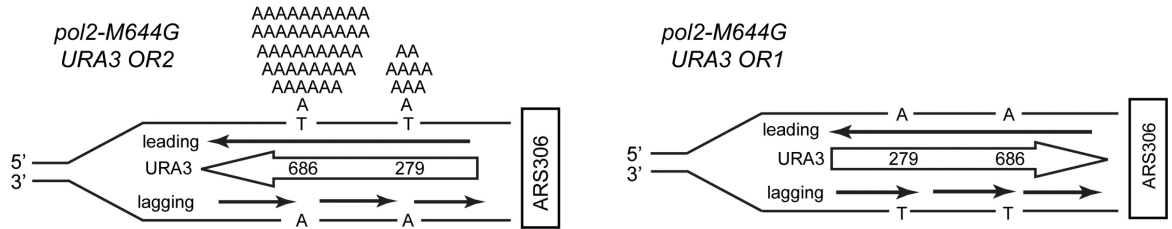
**Figure 5. Lack of strand bias of *URA3* mutations in the DBY747 *pol3-L612M msh2* strain at ARS1**

(A) Hot spot mutations in *URA3* observed in OR1 in the DBY747 *pol3-L612M msh2* strain. The *URA3* ORF (boxed arrow) is located ~600 bp to the left of ARS1 on chromosome 4 and is not drawn to scale. Strand specific mutation rates for each site were calculated as described in the text, and the leading and lagging strand hot spot mutation rates given on the far right are the sum of all hot spot mutations on that strand. (B) Hot spot mutations in *URA3* near ARS1 observed in OR2 in the DBY747 *pol3-L612M msh2* strain. The orientation of *URA3* is reversed from that in (A). See also Figure S7 and Tables S5 and S6.

**A**

		Mutation		Total		Leading:lagging mispair ratio (A to T : T to A)
		$\begin{matrix} T & \rightarrow & A \\ A & \rightarrow & T \end{matrix}$		$\begin{matrix} A & \rightarrow & T \\ T & \rightarrow & A \end{matrix}$		
		Mispair T:dTTP > A:dATP		M644G Pol $\epsilon$ bias 39:1		
<i>ura3</i> mutation	A279T	A686T	Total A to T	Total T to A		
OR2		T:dTTP location				
	Lead	Lead	Lead	Lag		
<i>pol2-M644G MSH2</i> <sup>+</sup>	10/75	44/75	61/75	1/75	61 : 1	
<i>pol2-M644G msh2</i> $\Delta$	0/81	0/81	2/81	4/81	1 : 2	
OR1		Lag		Lag		
	Lag	Lag	Lag	Lead		
<i>pol2-M644G MSH2</i> <sup>+</sup>	0/43	0/43	1/43	9/43	9 : 1	
<i>pol2-M644G msh2</i> $\Delta$	0/66	0/66	0/66	4/66	4 : 0	

**B**



**C**

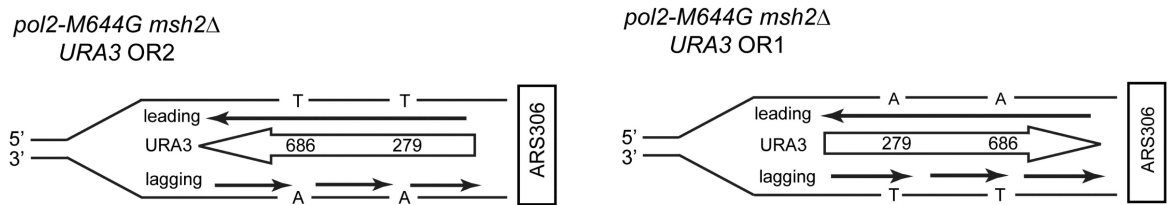


**Figure 6. Lack of *pol2-M644G* signature errors in MMR deficient strains**

(A) Mutational bias for A to T and T to A mutations in *pol2-M644G* and *pol2-M644G msh2* strains. The T:A to A:T mutation is shown above the 2 mispairs that cause the mutation. The signature bias exhibited by *pol2-M644G* is indicated (Pursell et al., 2007). The number of spontaneous A to T and T to A mutation events as well as hotspot mutations A279T and A686T in *pol2-M644G* and *pol2-M644G msh2* strains harboring *URA3* in orientation 1 (OR1) or in orientation 2 (OR2) are shown. The location of the T:dTTP mispair in the leading (lead) or lagging (lag) strand in each orientation is shown and the ratio of leading strand versus lagging strand mutations is given. (B) and (C) Schematic representation of the leading and lagging strand specific mutational events at A279 and A686 in *URA3* in OR1 or in OR2 in the *pol2-M644G* (B) and *pol2-M644G msh2* (C) strain.

**Table 1**

Reversion rates of *ura3-104* in two orientations (OR1 and OR2) in the S288C yeast strain carrying *pol3-L612M* in combination with mutations in different mismatch removal processes  
See also Figures S5 and S6.

Strain	Ura+ rate [ $\times 10^{-9}$ ] (95% CI)	CAG rate [ $\times 10^{-9}$ ] (95% CI)	Numbers of CAG : numbers of GAG+TCG+TTG+AAG
OR2 (T:G on lagging strand)			
WT	2.5 (1.7–3.3)	1.3 (0.9–1.7)	47 : 48
<i>pol3L612M</i>	22 (16–28)	21 (15–27)	103 : 4
<i>pol3L612M pol2-4</i>	20 (18–22)	19 (17–21)	122 : 8
<i>pol3L612M exo1</i>	140 (138–142)	132 (130–134)	116 : 7
<i>pol3L612M pol2-4 exo1</i>	440 (395–485)	419 (376–462)	120 : 6
<i>pol3L612M msh2</i>	399 (303–495)	396 (301–491)	117 : 1
<i>pol3L612M msh2 exo1</i>	488 (444–532)	488 (444–532)	124 : 0
OR1 (T:G on leading strand)			
WT	2.7 (2–3.4)	1.2 (0.9–1.4)	35 : 47
<i>pol3L612M</i>	4.0 (3.8–5.2)	2.4 (1.7–3.1)	57 : 36
<i>pol3L612M pol2-4</i>	3.5 (2.8–4.2)	3.5 (2.8–4.2)	121 : 0
<i>pol3L612M exo1</i>	22 (21–23)	15 (14–16)	84 : 48
<i>pol3L612M pol2-4 exo1</i>	206 (159–253)	206 (159–253)	123 : 0
<i>pol3L612M msh2</i>	917 (775–1059)	896 (758–1034)	124 : 2
<i>pol3L612M msh2 exo1</i>	1172 (942–1420)	1143 (901–1385)	118 : 3